

undoubtedly due to the phosphorescences from 9-NA and anthracene.

The phosphorescence decay curve of 9-NA was monitored at 685 nm (Figure 2 (II)), and the lifetime was solvent insensitive. (Observation at 760 nm did not give any better decay curve because of the much weaker intensity at this wavelength.) In Table I, the lifetimes of the phosphorescence and the $T' \leftarrow T_1$ absorption² of 9-NA are listed together with those of anthraquinone.¹¹ For 9-NA the lifetime of phosphorescence is slightly shorter than that of $T' \leftarrow T_1$ absorption. This may be due to the fact that the phosphorescence measured at 685 nm with a wide band-pass includes some emission from anthraquinone, as is obvious from the excitation spectrum (broken line shown in Figure 3). On account of the short triplet lifetime of anthraquinone (3.2 ms), the apparent lifetime may become shorter than the true phosphorescence lifetime of 9-NA. Unfortunately, the S/N ratio was too poor to resolve the observed decay curve into two components, i.e., the true triplet lifetimes of 9-NA and anthraquinone.

Discussion

It is well established that the phosphorescences in anthracenes are observed in the red-wavelength region ($\sim 14\,700\text{ cm}^{-1}$) and that the energy level of the lowest triplet state is hardly influenced by substitution.¹² As has previously been reported by one of us (S.H.),⁵ this is true even for such a substituent as a carbonyl group, which is expected to interact strongly with the anthracene moiety. Therefore, it is most reasonable to expect that 9-NA also exhibits phosphorescence in the same wavelength region as does anthracene. In fact, low-temperature luminescence from 9-NA was observed in the expected wavelength region. The assignment of this luminescence as phosphorescence from 9-NA is based on the following facts: (1) the excitation spectrum agrees well with the

absorption spectrum of 9-NA observed at 77 K; (2) the lifetimes determined from the decays of the phosphorescence and $T' \leftarrow T_1$ absorption are in reasonable agreement; (3) upon continuous irradiation, the phosphorescence intensity decreases owing to the photochemical consumption of 9-NA, which rules out the possibility of the phosphorescence being due to photoproducts; and (4) the phosphorescence spectral shape of 9-NA is characteristic of substituted anthracenes, i.e., the first three peaks are fused into a single broad band. Thus, it is unlikely that the observed phosphorescence is due to some anthracene derivative which might happen to be present as an impurity.

Taking these things into account, it is very surprising to note that, in their search for the phosphorescence from 9-NA, Snyder and Testa^{3,13} used an IP 21 photomultiplier whose spectral response suddenly drops above 650 nm and hence hardly spans the expected phosphorescence spectral range. Undoubtedly, therefore, their conclusion that no phosphorescence in 9-NA is observable is based on the insensitivity of their detection system and their failure to examine the proper spectral region. In addition, their assertion that the transient absorption assigned to the $T' \leftarrow T_1$ absorption of 9-NA in our previous paper² must be due to that of anthraquinone is utterly unfounded. While the lowest triplet state of 9-NA is expected to be of $\pi\pi^*$ character, the lowest triplet state of anthraquinone is of $n\pi^*$ character, and hence its lifetime cannot be as long as 17.7 ms. Actually, the measured phosphorescence lifetime of anthraquinone is only 3.2 ms, and the band maximum of the $T' \leftarrow T_1$ absorption of 9-NA is located at considerably longer wavelength than that of anthraquinone, as shown in Table I.

In conclusion, genuine phosphorescence of 9-NA has been observed and its lifetime has been measured. Previously reported failures to detect this luminescence are attributable to the use of an inappropriate photomultiplier and a failure to search in the proper spectral region.

Registry No. 9-NA, 602-60-8.

(11) Hamanoue, K.; Kajiwara, Y.; Miyake, T.; Nakayama, T.; Hirase, S.; Teranishi, H. *Chem. Phys. Lett.* **1983**, *94*, 276.

(12) McGlynn, S. P.; Azumi, T.; Kinoshita, M. "Molecular Spectroscopy of the Triplet State"; Prentice-Hall: Englewood Cliffs, NJ, 1969; p 286.

(13) Snyder, R.; Testa, A. C. *J. Phys. Chem.* **1979**, *83*, 3041.

Electrochemical Investigation of Photocatalysis at CdS Suspensions in the Presence of Methylviologen

James R. White and Allen J. Bard*

Department of Chemistry, The University of Texas, Austin, Texas 78712 (Received: June 7, 1984)

Addition of electron acceptors, such as methylviologen (MV^{2+}), resulted in enhanced photocurrents in photoelectrochemical (PEC) cells containing CdS powder suspensions. The variation of steady-state photocurrents with pH allowed the determination of band positions in aqueous electrolytes. The quasi-Fermi level for electrons (pH 14) was found to be at -0.81 , -0.76 , and -1.01 V vs. SCE for suspensions of CdS, CdS/RuO₂ (5%), and CdS/Pt (5%), respectively. Photocoulometric experiments, in which the total photogenerated charge (i.e., integrated photocurrent) was used to determine stability of semiconductor particles, are also reported. Turnover numbers for the CdS/catalyst suspensions were near 1 when sacrificial donors were not present; i.e., they are only stable toward decomposition in the presence of substances such as tartrate.

Introduction

The use of CdS colloids and suspensions as catalysts in several photosynthetic and photocatalytic reactions has been studied by a number of workers.¹⁻¹⁰ CdS is particularly interesting because

its band gap (2.4 eV) is such that it absorbs an appreciable fraction of light in the visible region. For photochemical applications of CdS, information about the particle energetics (i.e., the band positions) for CdS in contact with a solution and about the stability of the catalysts under long-term irradiation is very useful. A

(1) Frank, S. N.; Bard, A. J. *J. Phys. Chem.* **1977**, *81*, 1484.

(2) Spikes, J. *Photochem. Photobiol.* **1981**, *34*, 549.

(3) Darwent, J. R.; Porter, G. *J. Chem. Soc.* **1981**, *4*, 145.

(4) (a) Kalyanasundaram, K.; Borgarello, F.; Grätzel, M. *Helv. Chim. Acta* **1981**, *64*, 362. (b) Kalyanasundaram, K.; Borgarello, E.; Duonghong, D.; Grätzel, M. *Angew. Chem., Int. Ed. Engl.* **1981**, *20*, 987. (c) Borgarello, E.; Erbs, W.; Grätzel, M. *Nouv. J. Chim.* **1983**, *7*, 195.

(5) (a) Harbour, J.; Hair, M. *J. Phys. Chem.* **1977**, *81*, 1791. (b) Harbour, J.; Wolhow, R.; Hair, M. *Ibid.* **1981**, *85*, 4026.

(6) Matsumara, M.; Hiramoto, M.; Iehara, T.; Tsubomura, H. *J. Phys. Chem.* **1984**, *88*, 248.

(7) Rossetti, R.; Brus, L. *J. Phys. Chem.* **1982**, *86*, 4470.

(8) Kuczynski, J.; Thomas, J. K. *J. Phys. Chem.* **1983**, *87*, 5498.

(9) Meissner, D.; Memming, R.; Kastening, B. *Chem. Phys. Lett.* **1983**, *96*, 34.

(10) (a) Henglein, A. *Ber. Bunsenges. Phys. Chem.* **1982**, *86*, 241. (b) Henglein, A. *J. Phys. Chem.* **1981**, *86*, 2291.

number of methods have been used to elucidate the behavior of semiconductor suspensions. These include electron spin resonance,^{5a,11} photoelectrophoresis,¹² laser photolysis,¹³ conductivity,¹⁴ and luminescence measurements.^{7,10,15} Previous reports from our group discussed the use of electrochemical measurements in which photogenerated charge at semiconductor particles was collected at an inert metal electrode immersed in an irradiated suspension, e.g., of TiO₂.^{12,16,17} Enhanced photocurrent was observed in the presence of small quantities of an electron trapping agent, such as Fe³⁺ or Cu²⁺. We now extend the work to encompass CdS suspensions and also present a model and experimental results for photocoulometry of semiconductor suspensions in the presence of the electron acceptor (mediator) methylviologen (MV²⁺). Photocoulometry yields information about the relative rates of processes occurring under steady-state illumination such as the extent of the back reaction of photogenerated hole (h⁺) with the photoreduced acceptor and the extent of e⁻h⁺ recombination. Photoelectrochemical (PEC) cells containing MV²⁺ were used to determine the positions of the quasi-Fermi level for electrons, nE_F^* , for CdS and CdS modified with Pt and RuO₂ as a function of pH. These results are useful in predicting behavior of these photocatalysts for hydrogen production. Finally, photocoulometry allows the computation of turnover numbers (TN) for the catalysts during long-term illumination; these indicate the conditions under which CdS suspensions are stable toward photodecomposition.

Experimental Section

Preparation of Catalysts. CdS (Aldrich, 99%) was used in all experiments. Scanning electron microscopy revealed a grain size of approximately 0.1 μm . CdS/RuO₂ particles were prepared as previously described^{4c} with minor changes from a suspension of 1.0 g of CdS in 20 mL triply distilled water. A 7.5-mL sample of a 0.01 M RuCl₃ solution was added, and the suspension was stirred for 30 min, filtered, and washed with H₂O. The particles were dried in air at 70 °C for 30 min and subsequently annealed for 1 h at 300 °C in a N₂ atmosphere, then for 1 h at 300 °C in air. The resulting powder was 5% (w/w) RuO₂. CdS/Pt (5% w/w) was prepared by adding 2 g of CdS to 0.1 M sodium potassium tartrate (30 mL) and adjusting the pH to 4. A 6.1-mL sample of a 0.08 M solution of H₂PtCl₆ was added. The suspension was stirred and degassed with N₂ for 1 h and then irradiated. The powder was filtered, washed, and air-dried. Colloidal CdS was prepared by the addition of 10 mL of a 0.01 M stock solution of Cd(NO₃)₂ (Fisher Scientific) to 100 mL of a 0.1% poly(vinyl alcohol) (PVA, Aldrich M_R 86000). A 10-mL sample of a freshly prepared Na₂S (Alfa Products) solution was added all at once, resulting in a transparent yellow solution which was stable to flocculation for several weeks.

Chemicals. 1,1'-Dimethyl-4,4'-bipyridinium dichloride (methylviologen, MV²⁺, Sigma Chemicals) was added to suspensions from a freshly prepared 0.01 M stock solution. Details of the preparation and electrochemical behavior of FeB(OH)₂²⁺ (B is the macrocyclic ligand, 2,13-dimethyl-3,6,9,12,16-pentaazabicyclo-[12.3.1]octadeca-1(18),2,12,14,16-pentaene) have been described.¹⁸ All other chemicals were used as received without further purification, and all solutions were prepared with water that was triply distilled from permanganate.

Apparatus. The electrolysis cell was a two-compartment Pyrex cell divided by a fine porosity glass frit. One compartment housed

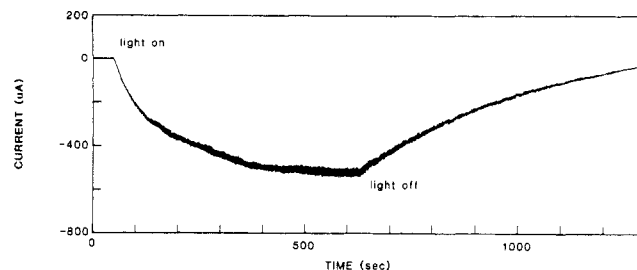


Figure 1. Photocurrent vs. time for CdS suspension. 1.0 M NaOH, 3.0 $\times 10^{-4}$ M MV²⁺, 100 mg CdS, Pt collector electrode (10 cm²) at -0.40 V vs. SCE.

TABLE I: Electron Acceptors and Steady-State Photocurrent at Irradiated CdS Suspensions

acceptor ^a	$E^{\circ'}$, V vs. SCE	i_{ss} , ^b mA
Cu ²⁺	+1.0	0
Fe ³⁺	+0.53	0
<i>p</i> -benzoquinone (BQ)	-0.12	0.2
FeB(OH) ₂ ²⁺ (pH 12.0) ^c	-0.79	0.8
Fe(CN) ₆ ³⁻	+0.22	1.8
Ru(NH ₃) ₆ ³⁺ (pH 10)	-0.2	1.2
MV ²⁺ (pH 14)	-0.69	1.1

^aInitial concentration of acceptor was 1.0 mM; pH was 7.0 unless otherwise indicated. ^bPhoto flux was $\sim 10^{18}$ photon s⁻¹ based on input power to the cell of 1.5 W. Electrode (Pt) area 10 cm². Electrode potential was maintained where oxidation of reduced form would occur at mass-transfer-controlled rate. ^cB is a macrocyclic ligand described in the Experimental Section.

the working electrode, a 10-cm² platinum gauze cylinder, and had a solution volume of 25 mL. Suspensions were stirred with a magnetic stirrer during the measurements. A saturated calomel reference electrode (SCE) was also fitted in this compartment. The second compartment contained a 21-cm² platinum counter-electrode. This cell was used in all experiments except those requiring in situ pH measurements. In that case, a larger cell (100-mL solution volume) with a port for placement of a Beckman combination pH electrode was used. The pH was adjusted by addition of either 1 M NaOH or 1 M HNO₃. All solutions were degassed with prepurified N₂ for 1 h before the experiments.

Irradiations were performed with a 3-kW xenon lamp (Christie Corp.) operated at 1.6 kW. A 10-cm water bath and a 390-nm cutoff filter were used to filter IR and UV irradiation, respectively. The lamp delivered 1.5 W of radiant energy to the cell, as determined with a radiometer/photometer (PAR Model 550-1). A Jarrell Ash monochromator with a 20-nm band-pass was used to obtain action spectra. All current-time curves were obtained with a Princeton Applied Research (PAR) Model 173 potentiostat/galvanostat, a PAR Model 175 universal programmer, and a Houston Instruments Model 2000 X-Y recorder.

Results

Collection of Photogenerated Charge. Illuminated suspensions of CdS, containing only supporting electrolyte (e.g., 1.0 M NaOH), produced anodic photocurrents at an inert metal electrode (collector electrode) immersed in the suspension. The magnitude of these photocurrents was low with a maximum of about 10 μA for a collector electrode of 10-cm² area. The addition of small quantities of an appropriate oxidant (electron acceptor) resulted in a significant increase in the observed photocurrent in a manner similar to that previously reported for TiO₂ suspensions.¹⁷ The magnitude of the observed photocurrent depended upon the concentration of the acceptor, the solution pH, the potential of the collector electrode, and the light intensity. In a typical experiment, a well-degassed suspension of CdS in a 1.0 mM MV²⁺ (pH 14) solution resulted in a maximum steady-state photocurrent (i_{ss}) of 1.1 mA. The collector electrode potential was held at a value at least 100 mV positive of the potential corresponding to the peak cathodic current, i_{pc} , for reduction of MV²⁺ as determined by cyclic voltammetry (CV) at a Pt disk electrode before the

(11) Jaeger, C. D.; Bard, A. J. *J. Phys. Chem.* **1979**, *83*, 3146.

(12) Dunn, W.; Aikawa, Y.; Bard, A. J. *J. Am. Chem. Soc.* **1981**, *103*, 3456.

(13) (a) Duonghung, D.; Borgarello, E.; Grätzel, M.; *J. Am. Chem. Soc.* **1981**, *103*, 4685. (b) Duonghung, D.; Ramsden, J.; Grätzel, M. *J. Am. Chem. Soc.* **1982**, *104*, 2977.

(14) Heinglein, A.; Lillie, J. J. *J. Am. Chem. Soc.* **1981**, *103*, 1059.

(15) Becker, W.; Bard, A. J. *J. Phys. Chem.* **1983**, *87*, 4888.

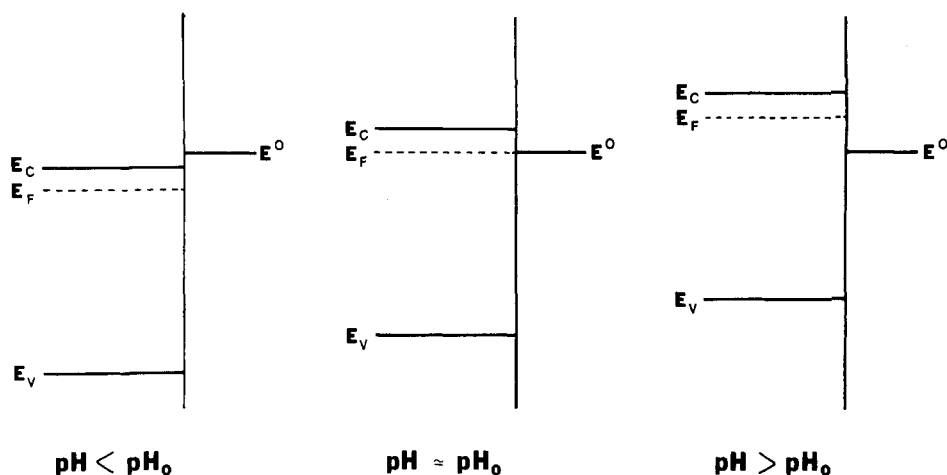
(16) Bard, A. J.; Pruiksma, R.; White, J. R.; Dunn, W.; Ward, M. D. *Proc.—Electrochem. Soc.* **1982**, *82-3*, 381-189.

(17) (a) Ward, M. D.; Bard, A. J. *J. Phys. Chem.* **1982**, *86*, 3599. (b)

Ward, M. D.; White, J. R.; Bard, A. J. *J. Am. Chem. Soc.* **1983**, *105*, 27.

(18) Chen, Y. D.; Bard, A. J. *Inorg. Chem.* **1984**, *23*, 2175.

SCHEME I



photochemical experiment. Thus, for MV^{2+} , i_{pc} occurred at -0.65 vs. SCE, and the collector electrode was held at -0.40 V. Under illumination MV^{2+} was photoreduced to MV^{+} at the CdS particles and subsequently reoxidized at the collector electrode, resulting in the observed anodic photocurrent (Figure 1). The photocurrent increased with time and reached a steady-state value, i_{ss} , after about 10 min. When the light was turned off, the photoreduced MV^{+} was electrolyzed back to the 2+ state; the current showed the typical first-order decay usually found in coulometric experiments with a rate determined by the mass-transfer characteristics of the cell. Values of i_{ss} obtained for several different acceptor species are given in Table I. The metal ions, Fe^{3+} and Cu^{2+} , which worked well as acceptors in TiO_2 suspensions, could not be employed for CdS because the metal ions rapidly displaced Cd^{2+} from the CdS causing discoloration of the CdS suspension. When these suspensions were irradiated, no photocurrent was observed. For most of the experiments, MV^{2+} was used as the electron acceptor because of the pH independence of its standard redox potential and its good stability.

The concentration of reduced acceptor in solution at any time, $C(t)$, could be obtained from the current according to the usual coulometry equation¹⁹

$$C(t) = i(t)/nFAm_0 \quad (1)$$

where the electrode reaction is $\text{R} - ne \rightarrow \text{O}$, F is the Faraday, and A the electrode area. The mass-transfer coefficient, m_0 was determined to be 8.0×10^{-3} cm/s by controlled potential coulometric reduction of a 1.0 mM MV^{2+} solution at the Pt electrode. Addition of CdS had no observable effect on the mass-transfer characteristics of the cell when the electrolysis was performed in the dark. Therefore, i_{ss} of 1.1 mA represents about 14% of the methylviologen in the reduced form (MV^{+}) at steady state for an initial concentration, C^* , of MV^{2+} of 1.0 mM. i_{ss} varied with C^* as shown by the points in Figure 2. In this figure, i_{ss} and C^* are divided by I , the incident photon flux. The ordinate then has units of electrons/photon and represents the efficiency of the process (number of electrons collected at the collector electrode divided by the number of incident photons). The photon flux was obtained by integration of the 1.5-kW xenon lamp output between 390 and 520 nm. Typical efficiencies (for $C^* = 1.0$ mM) are 0.36% for 1.0 M NaOH and 2.0% in the presence of donor, 0.1 M tartrate.

pH Effects. The effect of pH on i_{ss} for the CdS suspensions in MV^{2+} solution can provide information about the interfacial energetics.¹⁷ Since the standard potential, E° , of the $\text{MV}^{2+}/\text{MV}^{+}$ couple (-0.69 V vs. SCE) is independent of pH, any change in photocurrent as a result of a pH change must arise from changes in the energetics of the electrons photogenerated at the particle surface. For many semiconductors, as the pH increases the positions of the bands shift upward with respect to vacuum (i.e.,

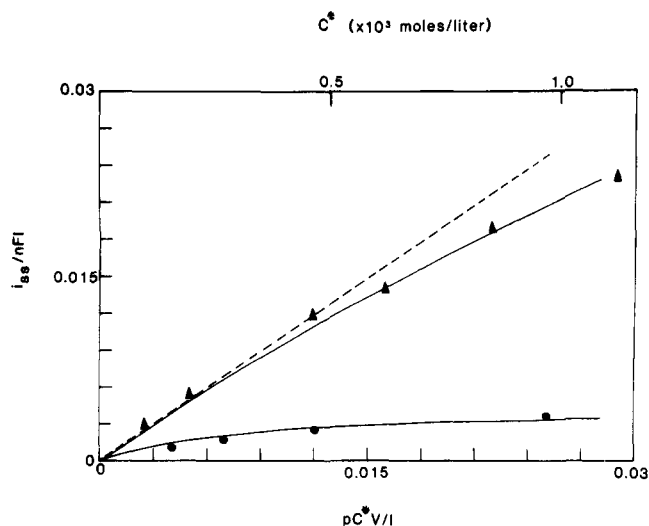


Figure 2. Dependence of i_{ss} on C^* . 1.0 M NaOH, 1.0 mM MV^{2+} , 100 mg CdS. \blacktriangle , with 0.1 M tartrate; \bullet , no tartrate. Solid curves from eq A9 (details given in text). Dotted line is the result of eq A9 in the absence of kinetics ($B = R = 0$).

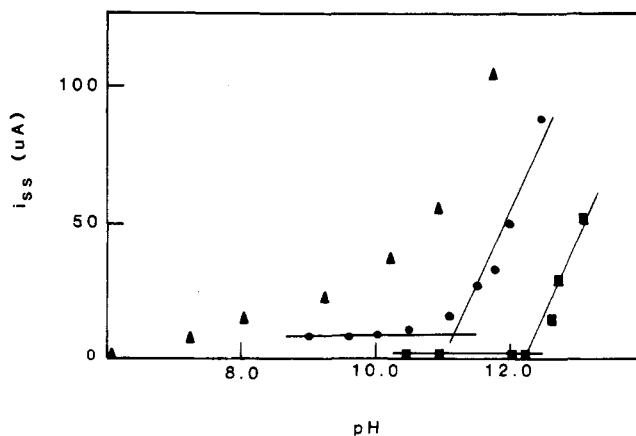


Figure 3. Effect of pH on steady-state current. 0.1 M KNO_3 , 100 mg catalyst, pH adjusted by addition of NaOH or HNO_3 . \bullet , CdS; \blacksquare , CdS/ RuO_2 (5%); \blacktriangle , CdS/Pt (5%).

the potential of photogenerated electrons becomes more negative or "more reducing" (Scheme I). At low pH, the conduction band edge lies positive of $E^\circ(\text{MV}^{2+}/\text{MV}^{+})$ and i_{ss} corresponds to the photocurrent observed in the absence of an acceptor. As the pH is increased, i_{ss} increases; the variation of i_{ss} with pH is shown in Figure 3. A threshold pH of 11.1 ± 0.1 could be identified for CdS catalysts. This pH value, termed pH_0 ,¹⁷ is the pH at which the onset of photocurrent mediated by the electron acceptor is observed. Below this pH the mediator made no contribution to

(19) Bard, A. J.; Faulkner, L. R. "Electrochemical Methods"; Wiley: New York, 1983; p 476.

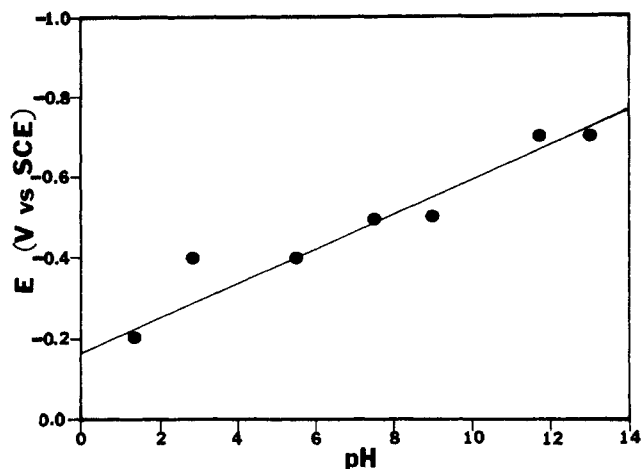


Figure 4. Onset of anodic photocurrent vs. pH for CdS suspension. 0.1 M KNO₃, pH adjusted with NaOH and HNO₃. 100 mg CdS.

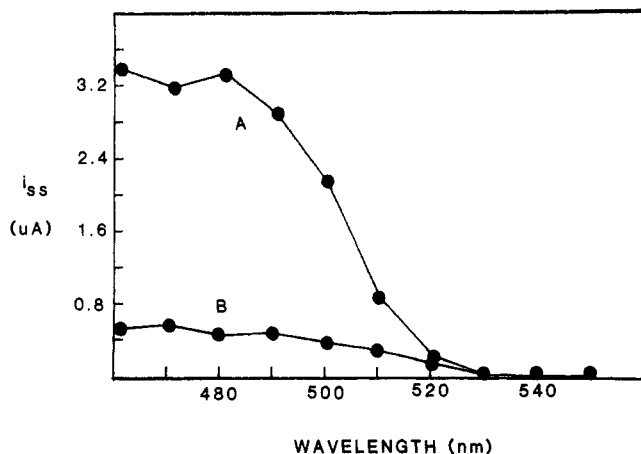


Figure 5. i_{ss} vs. wavelength for CdS (A) and CdS/RuO₂ (B). 1.0 M NaOH, 1.0 mM MV²⁺. Light intensity at 450 nm was 0.3 mW/cm² corresponding to 7×10^{14} photons/(s cm²).

the photocurrent. In the presence of 1.0 M tartrate, pH_0 shifted to 9.7. For CdS/RuO₂, pH_0 was found to be 12.2. For CdS/Pt determination of pH_0 was not as straightforward, since the slope in the region of pH 6–10 was less than in the case of CdS or CdS/RuO₂. pH_0 was estimated to be about 6, since in the region from pH 6–10, the solutions turned slightly blue, indicating that MV⁺ was present, and only very low photocurrents were observed with CdS/Pt in the absence of MV²⁺. Notice also that, as opposed to CdS alone, CdS modified with RuO₂ or Pt produced essentially no photocurrent at low pH or in the absence of an acceptor.

The shift in the band positions of CdS suspensions as a function of pH was also determined in the absence of an acceptor. The small anodic currents observed in this case correspond to charge transferred directly from the particles to the collector electrode. As the potential of the collector electrode is moved in a negative direction, the magnitude of the current decreases and a potential for the onset of current can be estimated. This onset potential shifted in a negative direction as the pH of the solution increased as shown in Figure 4. The slope of this line is 40 mV/pH unit, which is similar to the change in the flat-band potential as a function of pH reported for single crystals of CdS.^{20a}

Photoaction spectra of CdS and CdS/RuO₂ (Figure 5) were obtained by measuring i_{ss} as a function of irradiation wavelength. The values of i_{ss} are much smaller in this case because monochromatic light is employed. The only effect of RuO₂ was to lower the photocurrent due to light absorption by the RuO₂ on the CdS surface. The onset of photocurrent occurs at about 520 nm (2.4

TABLE II: Turnover Numbers (TN) for CdS Suspensions

amount of CdS, mg	coulombs available	measured	TN
11.3	15.1	16.9	1.1
0.57 ^a	0.77	0.75	1.0
10.2 ^b	13.6	14.4	1.1
9.62 ^c	12.8	10.1	0.8
7.86 ^d	10.50	253.0	>24.1
14.86 ^e	19.84	33.56	>1.7

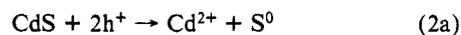
^a Colloidal CdS prepared from Cd(NO₃)₂ and Na₂S with poly(vinyl alcohol) as an antiflocculant; pH 12.0. ^b CdS/RuO₂ (5%). ^c 0.1 M acetate. ^d 0.1 M tartrate; experiment terminated before i_{ss} decayed to background. ^e 0.01 M Na₂S, pH 12.5. ^f 1.0 M NaOH and 1.0 M MV²⁺, unless otherwise indicated. Platinum collector electrode at -0.2 vs. SCE.

eV) in both cases, suggesting that there is no change in the band structure due to RuO₂ modification.

The monochromatic quantum efficiencies ($\lambda = 450$ nm) for CdS and CdS/RuO₂, defined as the number of electrons collected per incident photon, were 0.3% (CdS) and 0.03% [CdS/RuO₂ (5%)] under the conditions given in Figure 5.

CdS Stability. The steady-state currents under illumination listed in Table I (reached after about 10 min) remained essentially unchanged for at least 1 h but then decayed slowly with time over a period of several hours. The long-term stability of electron acceptor/suspension systems depended upon the stability of the mediator as well as the photocatalyst. BQ and FeB(OH)²⁺ gave moderate values for i_{ss} , but the photocurrent decayed to zero within 1 h because of decomposition of the mediator. This disappearance of the oxidized form of mediator was confirmed by cyclic voltammetry at a Pt disk electrode. Fe(CN)₆³⁻ decomposed after several hours because it is photochemically active at the wavelengths used for excitation. Moreover, an anodic current of 50 μ A was observed in the dark when Fe(CN)₆³⁻ was added to CdS suspension, probably because E^0 of the mediator is positive of the thermodynamic decomposition potential for CdS leading to some spontaneous oxidative decomposition of CdS producing Fe(CN)₆⁴⁻ in the dark.²¹ MV²⁺ and Ru(NH₃)₆³⁺ both exhibited reasonable stability toward decomposition; with these mediators the stability of the illuminated cell was limited by the photocatalyst.

Since the rate of electrolysis by the collector electrode is equal to the rate of photoreduction at the particle surface, at steady state it is possible to monitor the number of coulombs passed in long-term experiments by integration of i_{ss} and calculate a turnover number (TN) for the CdS catalysts. In a typical experiment 11.3 mg of CdS was added to the cell, i_{ss} was allowed to decay to negligible values, and the number of coulombs required to reoxidize the MV⁺ was monitored. If the photoreaction proceeds according to eq 2, then the photogenerated holes lead to decomposition of the



CdS with 2 F of charge passed to consume 1 mol CdS and liberate 1 mol of Cd²⁺. This would yield 15.1 C, if 11.3 mg of the catalyst were completely consumed. After several hours of irradiation, the photocurrent had decayed from its original steady-state value to negligible values and the initially yellow suspension became colorless with no sign of the particulate catalyst remaining. The 16.9 C passed represented a TN of 1.1 or complete consumption of the CdS catalyst. Turnover numbers determined in this way for several different catalysts and electrolyte solutions are given in Table II. Note that a TN of 1.1 was obtained for CdS/RuO₂ catalyst as well. These results suggest that essentially all photogenerated holes lead to decomposition of CdS in the absence of a sacrificial donor in solution and that, under our conditions, the RuO₂ deposits cannot effectively compete with the lattice sulfide for the capture of the photogenerated hole. Colloidal

(20) (a) Gomes, W. P.; Cardon, F. *Proc.—Electrochem. Soc.* 1977, 77-3, 120-131. (b) Watanabe, T.; Fujishima, A.; Honda, K. *Chem. Lett.* 1974, 897. (c) Ginley, D. S.; Butler, M. A. *J. Electrochem. Soc.* 1978, 125, 1968.

(21) Wilson, J. R.; Park, S. J. *Electrochem. Soc.* 1982, 129, 149.

systems with poly(vinyl alcohol) (PVA) as an antiflocculating agent also showed a TN of 1.0, so that oxidation of the alcohol does not effectively compete with the decomposition reaction either.

The only cases where a TN greater than one was obtained were when sacrificial donors were added to the solutions. The addition of 0.1 M tartrate to the cell gave rise to values of i_{ss} which were significantly larger than those obtained for an analogous mediator concentration in the absence of tartrate at the same pH (Figure 2). There was no observable decomposition of CdS after 40 h of irradiation in the presence of tartrate. i_{ss} had decreased to 75% of its initial value in this case, and a CV of MV^{2+} after termination of the experiment showed an analogous drop in MV^{2+} concentration, caused by decomposition of the mediator on this time scale. We also attempted to employ acetate ion as a hole scavenger, since it is known to decompose in the photo-Kolbe decarboxylation at a TiO_2 particle surface.²² However, for acetate, TN was 0.8, indicating no stabilization toward decomposition. Na_2S was also employed as a sacrificial agent. For a significant photoreduction of MV^{2+} to occur the pH was adjusted to 12.5. At this pH, however, there was a significant amount of dark reduction of MV^{2+} by sulfide ion resulting in a dark current of 200 μA . Under irradiation i_{ss} was 800 μA . When the experiment was terminated after several hours, a photocurrent of ca. 300 μA was observed with the dark reaction still accounting for 25% of the total current. At this time the catalyst was still visibly dispersed in the cell. The number of coulombs passed (corrected for the dark reaction) under these conditions indicates a TN > 1.7 in the presence of sulfide. $Ru(NH_3)_6^{3+}$ was employed as a mediator in long-term experiments as well. For a suspension of CdS at pH 10, containing 1.0 mM $Ru(NH_3)_6^{3+}$, a TN of 0.8 was obtained.

Discussion

The electrochemical behavior of CdS suspensions generally follows that of TiO_2 .¹⁷ CdS particles behave as microheterogeneous electrodes in which e^-h^+ pairs are generated by irradiation with light of greater than bandgap energy. In the absence of solution redox species, holes react with lattice S^{2-} and the photogenerated electrons can be collected at an inert metal electrode placed in the solution, resulting in anodic photocurrents. This process is relatively inefficient, however, probably because of e^-h^+ recombination, and low photocurrents are observed. Addition of small amounts of the oxidized form a redox couple results in a large enhancement of the photocurrent. This enhancement can be attributed to efficient scavenging of electrons by solution species.

Methylviologen was used as the acceptor in most experiments and has been reported to adsorb on the CdS surface.^{10b,13b} Since the presence of CdS had no observable effect on the electrolysis of MV^{2+} in the dark and since data were taken at steady state, the adsorption of MV^{2+} is probably not an important factor in the interpretation of the results. Enhanced photocurrents are produced with alternative acceptors (both neutral or anionic) so that enhancement in the presence of electron acceptors appears to be a general phenomenon. There are three major constraints to be considered in the selection of an acceptor species. First, aquated metal ions, such as Fe^{3+} and Cu^{2+} , cannot be used because they displace Cd^{2+} from the lattice, making the suspension inactive. When metals are in the form of more stable complexes, e.g., $Ru(NH_3)_6^{3+}$, the exchange of metal ions is slowed and stable photocurrents are produced. A second constraint is that $E^{o'}$ for the acceptor should be negative of the decomposition potential, E_D , for CdS, which is 0.08 V vs. SCE.²³ When $E^{o'}$ is positive of E_D , a dark anodic current can arise due to the spontaneous oxidation of the semiconductor by the acceptor (e.g., with ferricyanide). A third constraint is that the acceptor be stable to successive turnovers in a solution environment (usually basic) conducive to charge transfer between the semiconductor and the acceptor. For BQ and $FeB(OH)^{2+}$ photocurrents could be observed initially, but they decayed quickly because the acceptor species decomposed.

Photocoulometry Model. We now attempt to interpret the variation of the steady-state current in photocoulometry with the initial acceptor concentration, C^* (Figure 2). Several papers have addressed the kinetic processes in photoprocesses at semiconductor suspensions.^{16,24} The complexity of the mass transport and electron-transfer processes leads to equations which are difficult to apply to actual experimental systems with few adjustable parameters. Here we propose a model based on treating the system as a homogenous photochemical one and consider only the steady-state behavior. Thus the model is analogous to those used for coulometry with coupled chemical reactions¹⁹ with generation of electroactive product by photoreaction²⁵ and loss of product by homogeneous reactions and by bulk electrolysis.

We model the system with the following scheme:

(1) Light absorption by the semiconductor particles

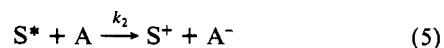


where S^* represents a photogenerated e^-h^+ pair.

(2) Recombination



(3) Electron capture by the acceptor, A



(4) Back reaction of the reduced acceptor



(5) Hole capture by a donor, D



(6) Lattice decomposition



For CdS particles this represents formation of $Cd^{2+} + S$.

(7) Oxidation of A^- at the electrode



where p is the coulometry cell constant, in s^{-1} [$p = m_0$ (electrode area)/ V] and was found to be $3.0 \times 10^{-3} s^{-1}$ by controlled potential reduction of MV^{2+} .

Details of the mathematical treatment and the resulting expressions are given in the Appendix. Briefly the steady-state concentration of A^- (i.e., MV^{+}) is calculated as a function of the experimental parameters I/pV and C^* [where I is proportional to the intensity of irradiation and C^* is the total (analytical) concentration of A], and the rate parameters $R = k_1/k_2$ and $B = k_3/(k_4D + k_5)$. The steady-state current, i_{ss} , is then obtained with the equation

$$i_{ss}/nFV = p[A^-] \quad (10)$$

Figures 6 and 7 illustrate calculations based on eq A9, showing the effect of the kinetic parameters on i_{ss} . In the absence of the back reaction ($B = 0$) and recombination ($R = 0$), the normalized current, i_{ss}/nFI , increases linearly (with a slope of 1.0) with the normalized initial concentration, pC^*V/I , for values less than 1.0. In this region $pC^* < I/V$ and the mediator is almost completely in the reduced form; under these conditions, i_{ss} is mass-transfer limited and equals $nFam_0C^*$. When $pC^*V/I > 1$, there is a sufficient excess of oxidized mediator that i_{ss} is limited by the light flux. Under these conditions, i_{ss}/nFI reaches a constant, light-limited value corresponding to an efficiency of 1.0.

An increase in the rate of the back reaction (parameter B) (Figure 6) has little effect at low values of pC^*V/I . The slope of the curve in this region is very similar to that in the absence

(24) (a) Curran, J. S.; Lamouche, D. *J. Phys. Chem.* **1983**, *87*, 5405. (b) Grätzel, M.; Frank, A. *J. Phys. Chem.* **1982**, *86*, 2964. (c) Albery, W. N.; Bartlett, P. N. *J. Electrochem. Soc.* **1984**, *131*, 315.

(25) Fitzgerald, J. M., Ed. "Analytical Photochemistry and Photochemical Analysis"; Marcel Dekker: New York, 1971; pp 145-153.

(22) Krautler, B.; Bard, A. J. *J. Am. Chem. Soc.* **1978**, *100*, 5985.

(23) Bard, A. J.; Wrighton, M. S. *J. Electrochem. Soc.* **1977**, *124*, 1706.

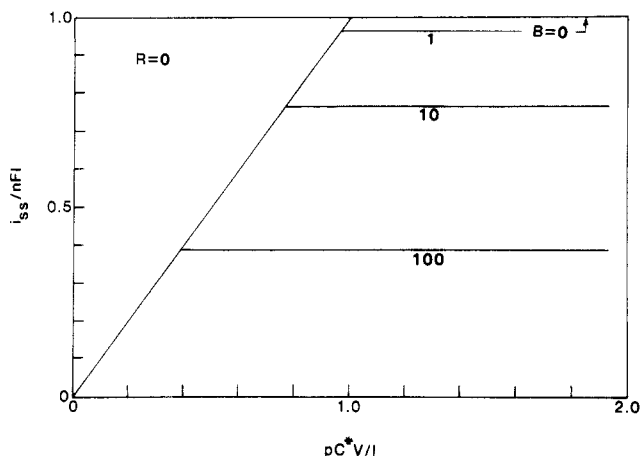


Figure 6. Theoretical variation of i_{ss} with C^* , based on eq A9. $R = 0$, $B = 0, 1, 10, 100$.

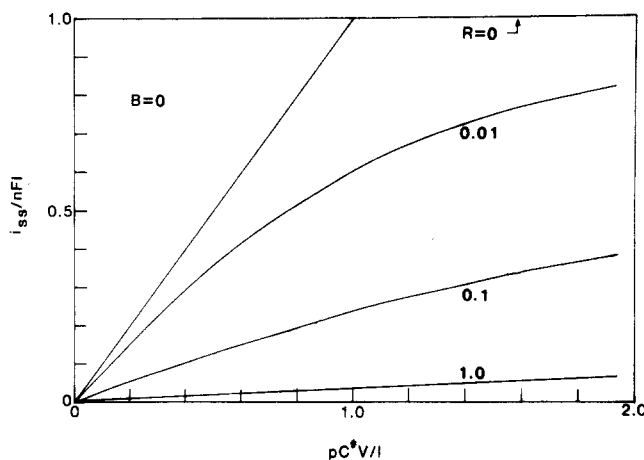


Figure 7. Theoretical variation of i_{ss} with C^* , based on eq A9. $B = 0$, $R = 0.01, 0.1, 1.0$.

of kinetics, and i_{ss} approaches the mass-transfer-limited value in spite of reaction 6. However, as pC^*V/I increases, the efficiency of the PEC limits at a nearly constant value, governed by the rate of reaction 6. The recombination (parameter R) (Figure 7) affects the initial slope as well as the limiting efficiency of the PEC.

The model (eq A9) when fitted to the experimental data (Figure 2, solid curves), can be used to estimate the relative rates of the different processes. In the absence of a donor, the best fit occurs for $R = 10^{-3}$ and $B = 10^6$ (for $D = 0$, $k_5 = 10^{-6}k_3$, from eq A11). In the presence of 0.1 M tartrate as a donor we estimate $B = 7.5 \times 10^3$ and $R = 10^{-3}$. Notice that the same value of R applies, as expected, for both cases. From eq A11 and the previous relation between k_5 and k_3 , we obtain $k_3 = 7.5 \times 10^3 k_4 D$, so that $k_4 D \gg k_5$. The rate of the back reaction (eq 6) is $k_3 S^+ A^-$, and the rate of the reaction of the hole with donor (eq 7) is $k_4 D S^+$ (which is equivalent to $k_3 S^+ / 7.5 \times 10^3$ based on our kinetic analysis). Under most of the experimental conditions employed here the steady-state concentration of A^- was near 10^{-4} M. Thus, the relative rates of these two reactions are similar, although the donor is present in nearly a thousandfold excess. These results also demonstrate that the donor effectively suppresses the decomposition reaction (since $k_4 D \gg k_5$), which agrees with the observed high turnover numbers. Note that the first three low concentration points for the tartrate system in Figure 2 lie on the curve for the solution of eq A9 in the absence of back reaction and recombination (i.e., $B = R = 0$). Thus, for these values of C^* the maximum efficiency is obtained, and losses are caused by the mass-transfer limitations of the cell and are primarily recombinative in nature.

A similar analysis can be carried out for the recombination parameter, $R = k_1/k_2$ which was found to be 10^{-3} . The rate of recombination (eq 4) is $k_1 S^*$ which is equivalent to $10^{-3} k_2 S^*$. Similarly the rate of electron transfer to the acceptor (eq 5) is given by $k_2 S^+ A^-$. The relative rates of these reactions depend upon

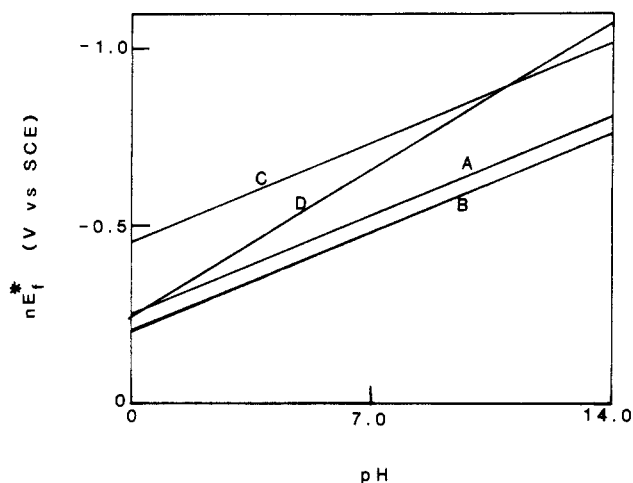


Figure 8. Variation of nE_F^* with pH for CdS suspensions. A, CdS; B, CdS/RuO₂; C, CdS/Pt. Curve D is the potential of the H⁺/H₂ couple.

the steady-state concentration of A. Again in the case of tartrate at small values of C^* , the acceptor is almost completely reduced and $A < 10^{-5}$ M. Under these conditions, essentially all loss in efficiency is attributable to recombination. When the steady-state value of A increases at large values of C^* , recombination becomes less important as the rate of eq 5 is enhanced.

pH Effects. The variation in i_{ss} with pH indicates a change in the band edge energies in the semiconductor with respect to those of the MV²⁺ system. Since $E^{o'}$ for methylviologen is independent of pH, the observed behavior indicates that changes must be occurring on the particle surface, thus changing the potential of the conduction band electrons. There are conflicting reports in the literature concerning the dependence of V_{fb} for CdS on pH.²⁰ However, our results seem to indicate that there is a pH dependence and that the behavior is similar to that observed for TiO₂ suspensions under similar experimental conditions.¹⁷

Adsorption of H⁺ or OH⁻ on the particle surface results in a shift of the semiconductor band positions in accordance with eq 11

$$E_F = E_F(\text{pH} = 0) - 0.04\text{pH} \quad (11)$$

where 0.04 is the slope of the line in Figure 4.

The CdS used was not intentionally doped; thus, the concentration of carriers was probably low, and the Fermi level in the dark was significantly positive of the conduction band. The Fermi level then splits into two quasi-Fermi levels under illumination, one for holes and one for electrons.²⁶ The energy level determined in these experiments is more adequately defined as the quasi-Fermi level for electrons under irradiation, nE_F^* . Under illumination, for the case $\text{pH} < \text{pH}_0$, the position of nE_F^* is such that it is more positive than E_{redox} and electron transfer does not occur (Scheme I, left). At $\text{pH} = \text{pH}_0$, nE_F^* is equivalent to E_{redox} , and electron transfer begins (Scheme I, center). As the pH is further increased, $\text{pH} > \text{pH}_0$ (Scheme I, right), the driving force for the reduction of MV²⁺ is also increased; this increases the rate of electron transfer. This is observed experimentally by the increase in i_{ss} with increasing pH. Knowledge of the value of E_F^* with eq 11 allows the determination of nE_F^* at any pH and is given by¹⁷

$$nE_F^* = E_{\text{redox}} - 0.04(\text{pH} - \text{pH}_0) \quad (12)$$

where E_{redox} is approximated by $E^{o'}$ for the MV^{2+/+} couple, -0.69 V vs. SCE.

The value of nE_F^* (pH 14) for CdS particulate suspensions was about -0.81 V vs. SCE. The values of nE_F^* (pH 14) for CdS/RuO₂ and CdS/Pt were -0.76 and -1.01 V vs. SCE, respectively. The band positions for the CdS/RuO₂ and CdS/Pt catalysts were assumed to shift with pH to the same extent as CdS catalysts (i.e., 40 mV/decade pH); since these forms show essentially no photocurrents in the absence of MV²⁺, we were unable to measure

the shift directly. A comparison of the nE_F^* values at different pH's with E_{redox} for the H^+/H_2 couple (Figure 8) suggests that the energies of the photogenerated electrons are marginal for hydrogen generation. CdS/Pt appears to be thermodynamically capable of producing H_2 for $\text{pH} < 11$. This agrees with recent results which show a similar dependence on pH of hydrogen production by CdS/Pt with formic acid as a donor.⁶ Unmodified CdS would be predicted to exhibit no H_2 evolution, except at low pH where CdS stability becomes a factor. This prediction is born out by results which show little or no H_2 production by CdS in the presence of EDTA, but significant quantities were produced for the CdS/Pt/EDTA system.^{3,5b} CdS/RuO₂ would not be expected to yield H_2 under any conditions, although in the presence of S^{2-} ion in solution, monograin CdS membranes modified with sputtered RuO₂ did yield H_2 with RuO₂ apparently functioning as a catalyst for H_2 evolution.⁹ However, in this case, the effect of S^{2-} ion on the CdS band energetics probably is important. The positive shift in nE_F^* due to RuO₂ deposits on the particle surface is in agreement with that observed for a positive shift of the flat-band potential of 0.5 V for a single crystal CdS electrode with a thin film of sputtered RuO₂.²⁷ In that case the positive shift was attributed to the formation of a Schottky barrier at the CdS/RuO₂ interface. The formation of a well-defined barrier on a particle surface does not seem likely. Band bending probably does not occur on particles with these dimensions and low doping density, since the dimension of the space-charge region would be on the order of the particle dimension. Additional evidence for the absence of band bending is given by the fact that the catalysts are completely consumed in the photolysis experiments. The mechanism of decomposition in the case of single-crystal CdS photoanodes is one in which an insulating layer of S^0 is formed at the surface of the crystal, preventing charge transfer.²⁸ This is a result of a significant space-charge region which allows e^- to be transferred to the bulk of the crystal and subsequently to the counterelectrode while the hole causes lattice oxidation, hence passivation at the surface. The mechanism for the decomposition of the particles appears to be different though, since dissolution of Cd^{2+} ions and elemental sulfur occurs, continually renewing the surface. Perhaps adsorption of ions onto the RuO₂ causes a shift in band edge potential. For example, the potential of zero charge of platinumized TiO₂ is more negative than that of TiO₂ alone; this has been ascribed to the specific adsorption of chloride ion on the TiO₂.¹²

Stability. The presence of the RuO₂ deposits, while influencing the energetics of the CdS particles, did not seem to stabilize them from photodecomposition, at least under the experimental conditions employed here. CdS also photodecomposes in the presence of PVA as an antiflocculating agent. Apparently only when a suitable sacrificial donor such as tartrate or sulfide is present was CdS stable to decomposition. H_2S in aqueous solutions also protects the CdS from decomposition.^{4c,29} The stability of the CdS in the presence of tartrate was reasonably good and photocurrents could be maintained for extended periods of time without decomposition of the catalyst. However, for long irradiation times decomposition of the mediator, MV^{2+} , became significant.

In assessing the turnover number for CdS in the presence of RuO₂, it is possible that O_2 is formed by reaction of photogenerated holes but that it reacts with MV^+ . This reaction, which produces MV^{2+} and superoxide ion, is quite rapid.³⁰ If this occurred the TN of ~ 1 would not necessarily indicate lack of O_2 formation. However, even when $\text{Ru}(\text{NH}_3)_6^{3+}$ is employed as an electron acceptor with CdS/RuO₂, a TN of about 1 was obtained. Since $\text{Ru}(\text{NH}_3)_6^{2+}$ does not react rapidly with O_2 , stabilization does not

appear to be likely in this case either.

Conclusions

Electrochemical measurements were shown to be useful in elucidation of the properties of irradiated CdS suspensions. Photocoulometry allowed estimation of the limiting steady-state efficiency of the suspensions. This approached 2.0% for 1 mM MV^{2+} , 0.1 M tartrate solutions. Photocoulometry also was useful in estimation of net turnover numbers and stability of the suspensions, and the effectiveness of different surface treatments and sacrificial donors in stabilizing the particle.

The variation of i_{ss} with pH showed that the band energies of CdS suspensions were functions of pH and allowed estimation of the potential of photogenerated electrons (~ -0.81 V vs. SCE at pH 14). Modification of the surface with RuO₂ or Pt changed the position of the energy levels.

Acknowledgment. We thank Dr. M. D. Ward for many helpful suggestions. The support of the National Science Foundation (CHE830466) and the Robert A. Welch Foundation is gratefully acknowledged.

Appendix

Based on the reaction scheme presented in eq 3–9, the following differential equations can be written:

$$dS^*/dt = I/V - k_1S^* - k_2AS^* \quad (\text{A1})$$

I represents the flux of photons absorbed by the CdS particles (in einsteins s^{-1}), and V is the volume of solution (assumed to be irradiated uniformly). S^* represents "excited" CdS particles (with e^-h^+ pairs), and A represents the molar concentration of species A. We assume that the sacrificial donor and semiconductor are

$$dS^+/dt = k_2S^*A - k_3S^+A^- - k_4DS^+ - k_5S^+ \quad (\text{A2})$$

present in large excess so that D and S remain constant over the time of the experimental measurement in which a steady state of A^- and i_{ss} are attained.

$$dA^-/dt = k_2S^*A - k_3S^+A^- - pA^- \quad (\text{A3})$$

At steady state, eq A1–A3 equal zero and A1 and A3 yield

$$I/V = k_1S^* + k_3S^+A^- + pA^- \quad (\text{A4})$$

An expression for S^+ can be obtained from (A2)

$$S^+ = k_2S^*A / (k_3A^- + k_4D + k_5) \quad (\text{A5})$$

and for S^* from (A1)

$$S^* = (I/V) / (k_1 + k_2A) \quad (\text{A6})$$

Substitution of (A5) and (A6) into (A4) yields

$$(I/V)[1 - k_1/(k_2A + k_1) - k_2k_3A^-A / ((k_3A^- + k_4D + k_5) \times (k_2A + k_1))] = pA^- \quad (\text{A7})$$

An equation in terms of A^- can be obtained from (A7) and the material balance

$$A + A^- = C^* \quad (\text{A8})$$

to yield

$$BA^{-3} + (1 - B(C^* + R))A^{-2} - (I/pV + C^* + R)A^- + (I/pV)C^* = 0 \quad (\text{A9})$$

In this equation the rate constants have been grouped to obtain two parameters, R and B . R is a measure of the relative im-

$$R = k_1/k_2 \quad (\text{A10})$$

$$B = k_3/(k_4D + k_5) \quad (\text{A11})$$

portance of the extent of recombination (eq 4) and reduction of A by a conduction band electron (eq 5). B is a measure of the relative extent of the back reaction of a hole with the reduced acceptor (eq 6) and of holes in decomposition of semiconductor and reaction with D .

(27) Gissler, W.; McEvoy, A. J.; Grätzel, M. *J. Electrochem. Soc.* **1982**, *129*, 1733.

(28) (a) Ellis, A. B.; Kaiser, S. W.; Wrighton, M. S. *J. Am. Chem. Soc.* **1976**, *98*, 6855. (b) Gerischer, H.; Mindt, W. *Electrochim. Acta* **1968**, *13*, 1329.

(29) Thewissen, D. H. M. W.; Tinneamans, A. H. A.; Eeuwhorst-Reinten, M.; Timmer, K.; Mackor, A. *Nouv. J. Chim.* **1983**, *7*, 191.

(30) Patterson, L. K.; Small, R. D.; Scaiano, J. C. *Radiat. Res.* **1977**, *72*, 218.

Equation A9 is solved for A^- , for given values of the experimental variables I/Vp and C^* , and appropriate values of R and B . In the experiments here the light intensity, and hence I/Vp , was held constant. Thus by inputting values for C^* we can observe changes in the value of A^- as a function of the kinetic parameters. A^- is, of course, related to i_{ss} by eq 10 and is equivalent to $i_{ss}/nFVp$. For convenience we have divided C^* and the resulting values of

A^- by the constant term I/Vp . This results in two dimensionless terms i_{ss}/nFI and pC^*V/I . As we mentioned earlier expressing the current this way is advantageous, since it is an expression of the efficiency of our system.

Registry No. MV²⁺, 1910-42-5; BQ, 106-51-4; FeB(OH)²⁺, 47176-02-3; Fe(CN)₆³⁻, 13408-62-3; Ru(NH₃)₆³⁺, 18943-33-4; CdS, 1306-23-6; RuO₂, 12036-10-1; Pt, 7440-06-4; KNO₃, 7757-79-1.

Fourier Transform Numerical Analysis of the Long-Range Proton Hyperfine Coupling in Nitroxide Radicals

P. Trousson and Y. Lion*†

Department of Physical Chemistry, The University, Leicester LE1 7RH, U.K. (Received: July 17, 1984; In Final Form: October 30, 1984)

A study of long-range proton coupling in nitroxide radicals has been performed with a numerical analysis program using the Fourier transform technique. The present method provides a means for further identification of radicals which is particularly useful for species that are otherwise indistinguishable. The superhyperfine structure of piperidine and pyrrolidine-1-oxyl derivatives, showing γ -nuclei coupling constants as small as 0.2 G, has been brought out. The results are in good agreement with those obtained by other resolution-enhancement methods.

Introduction

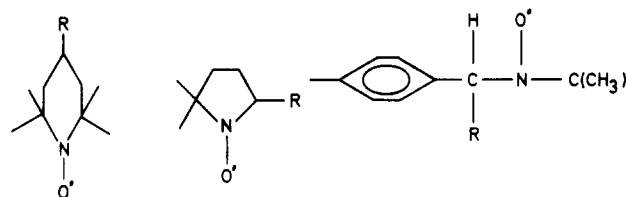
This study presents clear evidence of the potential of a post-experimental resolution-enhancement method. The technique, detailed in ref 1, is based on Fourier transform properties and consists of summing higher derivatives of the ESR signal and narrowing the line by changing the line shape function from Lorentzian to Gaussian. This method, which already proved to be helpful^{2,3} in solid matrices, is now applied to nitroxide radicals obtained by the spin-trapping method. The spin traps are extensively used to convert short-lived radicals into stable spin adducts by addition. This stabilization allows the detection and identification of the short-lived radicals if the structure of the spectrum is sufficiently resolved. It is unfortunately not the case when nitron spin traps are used; depending on the radical trapped, the nitron spectra exhibit splitting constants slightly different in magnitude, but the general structure of the spectra remains a six-line pattern. The information due to the superhyperfine (shf) interactions arising from nuclei three or four σ bonds away from the unpaired electron must be extracted from the line width of the observed lines.

We demonstrate in this work that the postexperimental data processing enables the observation of long-range nuclei interactions, with splitting constants as small as 0.2 G.

Study of such shf interactions on 4-R-2,2,6,6-tetramethylpiperidine-1-oxyl and 2-R-5,5-dimethyl-1-pyrroline N-oxide has already been performed by Mossoba et al.⁴ with another resolution-enhancement method. Both results are in good agreement, although, in some cases, our spectra exhibit even higher resolution, and our hyperfine structure (cepstral) analysis provides, in every case, precise hyperfine splitting constants.

Experimental Section

4-R-2,2,6,6-Tetramethylpiperidine-1-oxyl and 5,5-dimethyl-1-pyrroline N-oxide (DMPO) were purchased from Aldrich Chemical Co. and *N-tert*-butylphenylnitron (PBN) from Eastman Kodak Co. Purification of DMPO was carried out according to the procedure of Buettner and Oberley.⁵ Me₂SO and D₂O (99.75%) were obtained from Merck Co., and H₂O₂ (30 vol.%) was acquired from UCB (Belgium). Dilute aqueous solutions of



PIPERIDINE-
1-OXYL

PYRROLIDINE-
1-OXYL

N-BUTYL-
PHENYLNITRON

TEMPO R = H R = CH₃, OH, OD, COOH
 TEMPOL R = OH
 TEMPAMINE R = NH₂
 TEMPONE R = O

10⁻⁴ M of the stable nitroxide radicals were used, and dissolved oxygen was removed by bubbling nitrogen gas prior to the EPR measurements. The methyl adduct of DMPO was prepared by the UV photolysis of 30% H₂O₂ in an aqueous solution of DMPO (0.1 M) containing Me₂SO. COOH-DMPO was formed by the UV photolysis of an aqueous solution containing DMPO (0.1 M), sodium formate (1 M), and H₂O₂. The OH and OD adducts were generated by the photolysis of H₂O and D₂O solutions containing DMPO and H₂O₂.

- (1) Trousson, P.; Rinne, M. *Rev. Sci. Instrum.*, in press.
- (2) Symons, M. C. R.; Trousson, P. *Radiat. Phys. Chem.* **1984**, *23*, 127.
- (3) Maj, S. P.; Symons, M. C. R.; Trousson, P. *J. Chem. Soc., Chem. Commun.*, in press.
- (4) Mossoba, M. M.; Makino, K.; Riesz, P.; Perkins Jr., R. C. *J. Phys. Chem.* **1984**, *88*, 4717.
- (5) Buettner, G. R.; Oberley, L. W. *Biochem. Biophys. Res. Commun.* **1978**, *83*, 69.
- (6) Kirmse, D. W. *J. Magn. Reson.* **1973**, *11*, 1.
- (7) Windle, J. J. *J. Magn. Reson.* **1981**, *45*, 432.
- (8) Brière, R.; Lemaire, H.; Rassat, A.; Dunand, J.-J. *Bull. Soc. Chim. Fr.* **1967**, 4479.
- (9) Krellick, R. W. *J. Chem. Phys.* **1967**, *46*, 4260.
- (10) Bordeaux, D.; Lajzerowicz, J. *Acta Crystallogr., Sect. B* **1974**, *B30*, 790.
- (11) Heller, C.; McConnell, H. M. *J. Chem. Phys.* **1960**, *32*, 1535.
- (12) Lajzerowicz, J. *Acta Crystallogr., Sect. B* **1968**, *B24*, 196.
- (13) Berliner, L. J. *Acta Crystallogr., Sect. B* **1970**, *B26*, 1198.
- (14) Mao, S. W.; Kevan, L. *Chem. Phys. Lett.* **1974**, *24*, 505.
- (15) Harbour, J. R.; Chow, V.; Bolton, J. R. *Can. J. Chem.* **1974**, *52*, 3549.
- (16) Lai, C. S.; Piette, L. H. *Arch. Biochem. Biophys.* **1978**, *190*, 27.
- (17) Kasai, P. H.; McLeod Jr., D. *J. Phys. Chem.* **1978**, *82*, 619.

* Institut de Physique (B5), Université Liège, Sart-Tilman, 4000 Liege, Belgium.